

PAPER • OPEN ACCESS

## Optical fibre sensing for fast hotspot detection in SFCLs

To cite this article: Arooj Akbar *et al* 2020 *Supercond. Sci. Technol.* **33** 115003

View the [article online](#) for updates and enhancements.



**IOP | ebooks™**

Bringing together innovative digital publishing with leading authors from the global scientific community.

Start exploring the collection—download the first chapter of every title for free.

# Optical fibre sensing for fast hotspot detection in SFCLs

Arooj Akbar<sup>1</sup> , Zhisheng Yang<sup>2</sup> , Sheng Wang<sup>2,3</sup>, Luc Thévenaz<sup>2</sup> and Bertrand Dutoit<sup>1</sup>

<sup>1</sup> Applied Superconductivity Group, École polytechnique fédérale de Lausanne, Lausanne, Switzerland

<sup>2</sup> Group for Fibre Optics, École polytechnique fédérale de Lausanne, Lausanne, Switzerland

<sup>3</sup> State Key Laboratory of Information Photonics & Optical Communications, Beijing University of Posts and Telecommunications, Beijing, People's Republic of China

E-mail: [zhisheng.yang@epfl.ch](mailto:zhisheng.yang@epfl.ch)

Received 20 May 2020, revised 28 July 2020

Accepted for publication 24 August 2020

Published 21 September 2020



CrossMark

## Abstract

The health monitoring of superconducting fault current limiters (SFCL) is important for their large-scale exploitation in HVDC grids protection. The intrinsic non-homogeneity of critical current along the superconductor length can cause localized points of heating, called hotspots, in the SFCL device which can lead to device damage. In this paper we propose to use an extremely simple and cost-effective technique based on all-fibre Mach-Zehnder interferometers for hotspot detection in SFCLs, where the measurement arm of the interferometer is integrated with the SFCL and the reference arm remains in ambient. The system only consists of a laser, two optical fibre couplers and a photo detector. By studying the acquired interference patterns, even singular hotspots within the entire conductor length, can be informed in few milli-seconds, which is the fastest and most sensitive demonstration to the best of our knowledge that meets the SFCL requirement for fast hotspot detection.

Keywords: SFCLs, superconductivity, hotspots, optical fibre sensing

(Some figures may appear in colour only in the online journal)

## 1. Introduction

The grid is evolving as renewable energy generation is gradually taking more of a forefront in energy contribution. At present, HVDC links connect offshore renewable energy generation to the distribution grid; with increasing renewable energy generation the grid will gradually transform into a meshed HVDC grid. The protection mechanisms that work for AC grids will not be suited to address the protection of a low inertia meshed HVDC grid where the current lacks zero crossings and fault currents can reach extremely high values within 10 ms [1, 2]. Several studies have shown that resistive superconductive fault current limiters (SFCLs) are promising

candidates to provide selective protection for HVDC grids with their swift transition to resistive state in the presence of high currents [3, 4]. The high cost of SFCLs is one of the major impediment in employing this solution. The calculations for Eccoflow conductor with a limitation electric field of  $50 \text{ V m}^{-1}$  (50 ms) showed prohibitive costs of 200 €/kA/m [5]. The European Union project FastGrid aims at improving the REBCO tape architecture by increasing the limitation electric field with the overall goal of making a low length economically feasible SFCL device [6]. The optimized REBCO conductor will be used to make a high voltage DC SFCL module ( $\approx 1.5 \text{ kA}$ – $50 \text{ kV}$ ) operated at 67 K. The module will be equipped with an optical fibre sensing based health monitoring system to detect hotspots, which will be presented in this paper. Since the research presented in this paper is carried out in the framework of the FastGrid project, emphasis is placed on a DC device for HVDC grids. It should be noted, however, that the hotspot detection technique for SFCLs outlined in this paper can be employed in many high temperature



Original content from this work may be used under the terms of the [Creative Commons Attribution 4.0 licence](https://creativecommons.org/licenses/by/4.0/). Any further distribution of this work must maintain attribution to the author(s) and the title of the work, journal citation and DOI.

superconductor (HTS) applications and power devices. Like all superconducting systems, SFCLs need to be protected from their primary source of failure: hotspots. Hotspots are a consequence of the inherent material inhomogeneity present in coated HTS which are used in SFCLs. For Fastgrid conductors, Theva has optimised their production processes to limit the variation in critical current by less than or equal to 10%, which can be observed in their TapeStar measurements [7]. This material inhomogeneity produces an upper and lower bound on the local critical current ( $I_c$ ) along the HTS tape. This critical current, therefore, can be understood to lie in a band ranging from minimum critical current value ( $I_{c\_min}$ ) to the maximum critical current value ( $I_{c\_max}$ ), with different points along the superconductor transitioning to resistive state at different critical values. Under normal SFCL operation, the operating current ( $I_O$ ) level is below the minimum  $I_c$  i.e. ( $I_O < I_{c\_min}$ ), so that the entire superconductor is in superconducting state and features zero resistance. However, when a clear fault current develops, i.e. the operating current is beyond the highest  $I_c$  ( $I_O > I_{c\_max}$ ), the superconductor transitions uniformly from superconducting state to resistive state. It should be noted that the uniform transition may only occur if the electric field applied ( $E$ ) is greater than the critical electric field ( $E_q$ ), (i.e.  $E > E_q$ ), to ensure a homogenous quench as explained in Kraemer *et al* [8]. This sharp increase in resistance restricts fault currents and allows for further protective actions to be taken, such as opening the associated circuit breaker or diverting the current to a parallel circuit path with the desired higher impedance. The problem of hotspots, however, can occur when the operating current level is in between the bounds  $I_{c\_min}$  and  $I_{c\_max}$ , so that only few points or even a singular point in the superconductor may transition to resistive state. Such local transitions propagate by means of joule heating created by the initial normal zone with an extremely slow normal zone propagation velocity (NZPV) [9]. This puts HTS applications at a risk of high localized temperatures and irreversible material degradation in the event of a hotspot.

In a SFCL device, thermal runaways arise and eventually damage the device if hotspots go undetected for more than a few ms. This time allowance to react before device degradation varies according to the conductor architecture, like thermal stabilizer, substrate material and presence of current flow diverter (CFD) which varies in order to increase protection and decrease cost [10,11]. For conductors like the Eccoflow conductor with low electric field, the longer conductor lengths required increase the cost as well the reaction time to  $\sim 50$  ms. The conductors manufactured for the Fastgrid project, however, are designed to have a limitation field of  $>100 \text{ V m}^{-1}$  which is much higher than Eccoflow conductor. This decreases the conductor lengths required, the cost and the available timeframe to detect a hotspot to  $\sim 30$  ms. The highly localized hotspots and fast response requirements make hotspot detection a challenge. In addition, the high voltage environment presents a difficulty by forbidding electronic detection methods. Currently, grids use a current threshold to aid their decision-making process of opening the breaker to protect SFCLs; this is an extremely inefficient and non-selective

way to deal with high currents as the DC breakers are opened even when there is no hotspot. Currently no hotspot detection technique is capable of catering to the quick hotspot detection requirement in SFCLs. A hotspot detection technique with extremely fast response is therefore very desirable for SFCLs exploitability.

Optical fibre sensing is an attractive solution to detect hotspots in SFCLs because optical fibres are capable of working in high voltage environments and offer numerous advantages of being inexpensive, light-weight and chemically inert. Optical fibres can be seamlessly integrated in structures with a minimal impact on the host material, and various optical fibre sensing techniques enable measuring physical quantities such as temperature and strain along an optical fibre. Distributed optical fibre sensing using Rayleigh backscattering has been proposed and patented for hotspot detection in high temperature superconductors [12]. Although Rayleigh backscattering based techniques are capable of providing the location of the hotspot within the superconductor, the rather slow measurement speed ( $>100$  ms measurement time) critically hinders such techniques being used for the SFCL protection, which require a short measurement time (10–30 ms). While Rayleigh backscattering techniques are not fundamentally fast enough to protect a SFCL device, other quasi-distributed optical fibre sensing techniques like fibre Bragg gratings (FBG) present the disadvantage of information loss between the effective sensing locations [13].

In this paper, a Mach-Zehnder Interferometer based optical fibre sensing technique for extremely fast detection of hotspots within 10 ms is presented. Compared with Rayleigh scattering based techniques, the MZI method presents similar sensitivity, but is faster in terms of response and more cost effective in terms of setup. It is also worth mentioning that, although Rayleigh scattering techniques are advantageous in providing locations of hotspots, such feature is not needed for SFCL protection. The MZI technique is sufficient for informing about the presence of a hotspot quickly and economically. The technique presented in this paper provides a selective way to protect SFCLs, allowing the circuit breakers to open only in the case of a real hotspot by informing with certainty the existence of a hotspot.

This technique has been developed and filed as provisional patent by EPFL under the EU FastGrid project, with the full patent filing underway, the reference for which will be soon discoverable [14]. The FastGrid SFCL module will have optical fibre integrated along the conductor length for hotspot monitoring.

## 2. Mach-Zehnder principle and configuration

### 2.1. Configuration

The structure of MZI used in the study is shown in figure 1. The light from a narrow-linewidth laser is split into two branches: the upper one is integrated with the SFCL and serves as the signal branch, while the lower one acts as the reference branch. A device to adjust the polarization is present on the reference arm and under optimum conditions the light polarizations in both

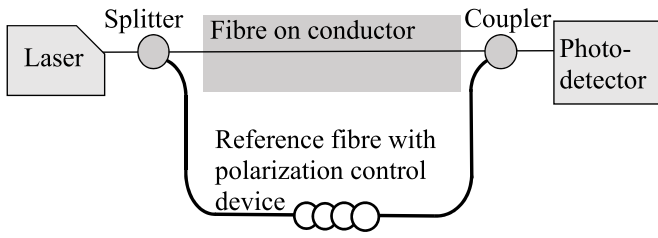


Figure 1. The Mach-Zehnder configuration.

branches are well aligned at the coupler. The lighthwaves transmitted through the two branches are recombined and converted into an electric signal via a photo detector. This output from the detector is an inteferece pattern with a phase dependent upon change in temperature and strain in the conductor; this property is used to detect hotspots.

### 2.2. Working principle

The analysis presented makes use of the variables below:

$\phi_{12}$	Initial phase shift between the two light paths
$\Delta\phi_H$	Phase shift due to hotspot and ambient factors
$\varepsilon$	Mechanical strain in the optical fibre
$\Delta T$	Temperature change due to the hotspot
$n$	Optical fibre refractive index
$\alpha_O$	Thermal expansion coefficient of the optical fibre
$\xi$	Thermo-optic coefficient of the optical fibre
$\rho_a$	Photo-elastic coefficient of the optical fibre

The recomobined electric signal output from the detector (i.e. the interference pattern) can be expressed as:

$$Interference\ Pattern \propto [1 + \cos(\phi_{12} - \pi + \Delta\phi_H)] \quad (1)$$

where  $\Delta\phi_H$  depends on the change in strain ( $\Delta\varepsilon$ ) and temperature ( $\Delta T$ ) as expressed in equation (2) [15]. Together, the two temperature and strain dependent phenomena affect the MZI response sensitivity which will be further addressed in section 4.3.

$$\Delta\phi_H \propto (\{1 - \rho_a\} \Delta\varepsilon + [\alpha_O + \xi] \Delta T) \quad (2)$$

When there is no hotspot in the superconductor, both  $\Delta\varepsilon$  and  $\Delta T$  are caused by environmental perturbations (environmental temperature variation and acoustic noises), resulting in a slow variation of  $\Delta\phi_H$ , so that the interference pattern shows slow fluctuations that do not exhibit a significant pattern. In the presence of a hotspot, the local heating gives rise to a temperature increment ( $\Delta T$  with positive sign) at the corresponding fibre position, meanwhile the local thermal expansion of the Hastelloy imposes a local elongation ( $\Delta\varepsilon$  with positive sign) of the optical fibre. This can result in a significant and continuous increment of  $\Delta\phi_H$ , from 0 to  $2\pi$ , within few ms, as the temperature of the hotspot increases sharply. Due to this  $\Delta\phi_H$  change, at the detector output the interference pattern manifests as continuous, periodic amplitude variations between 0 and 1 (normalized), with a frequency dependent upon the rate of temperature change; this

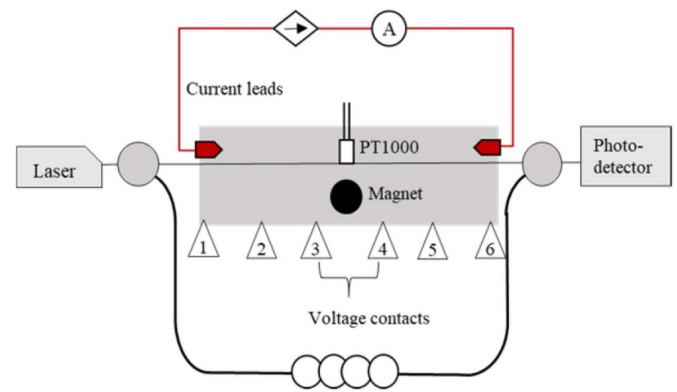


Figure 2. Experiment schematic.

is interpreted as the presence of (at least) a single hotspot. It is important to explain here, that the response to a hotspot and uniform transition varies in terms of frequency, i.e. the response will be higher in frequency in the latter case.

### 3. Experimental setup

Figure 2 shows the experiment schematic which comprises an optical fibre integrated along the length of a 30 cm long, 12 mm wide superconductor by means of STYCAST® 2850FT. STYCAST® is used because of its suitable thermal properties at cryogenic temperatures; its thermal expansion coefficient at 77 K is  $-0.43\%$  which is close to the value for ReBCO tapes,  $-0.23\%$ , leading to lower thermal stresses between the HTS tapes and the adhesive [16]. The adhesive is prepared with the right amount of catalyst to ensure a hard finish which creates a strong coupling between the optical fibre and the superconductor; this leads to a good mechanical and thermal response. The importance of optical fibre integration will be discussed in detail in section 4.4.

A 10 mm diameter,  $\sim 700$  mT permanent magnet pair is placed in close proximity at the centre of the sample to decrease the local critical current. The percentage decrease in the critical current in a perpendicular field of 700 mT can be estimated by the Kim-model which comes out to be around 80% for this experiment [17]. This creates a weak point, with a known location, for temperature and voltage monitoring. A PT1000 temperature sensor is placed on the conductor, in close proximity to the magnet. Voltage taps are added along the length of the superconductor tape for measuring the voltage in the hotspot regime and also in the adjacent segments to study the propagation of the transition. The laser wavelength used is 1550 nm, and a commercially available photodetector (Thorlabs PDB420C) is present at the MZI output. The sample is cooled to 77 K or may be further cooled to 67 K. Current is applied to the sample by means of a DC current pulser. Current through the sample and voltages around the weak point as well as along the sample length are measured. The MZI output and the PT1000 temperature are also acquired.

The 3D schematic of the experiment in figure 3 showcases the tape architecture used in these experiments. The figure also

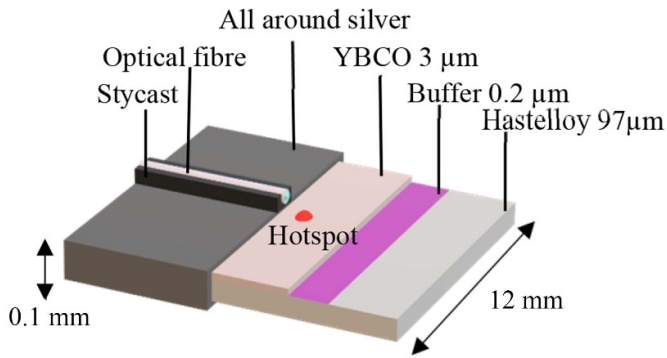


Figure 3. Experiment 3D cross-section.

explains how STYCAST<sup>®</sup> is used to integrate the fibre along the HTS tape. This 3D schematic does not show the thermal stabilizer, however, the experiment has also been conducted on the FastGrid conductors thermally stabilized by the addition of 500  $\mu\text{m}$  Hastelloy. In the case of thermally stabilized HTS tapes, the experiments were carried out by placing the optical fibre on either side.

## 4. Results and discussion

### 4.1. Experiment results for no hotspot

For this experiment 170 A is applied to the sample as shown in blue in figure 4(a). The voltage around the weak point,  $v_{3-4}$ , (voltage between contact 3 and 4 shown in figure 2) remains zero, signifying there is no hotspot in the sample. This is confirmed by the PT1000 temperature measurement which shows no temperature change. The interference pattern observed in the MZI output (red curve in figure 4(a)) shows fluctuations, attributed to variations in environmental factors like slowly varying temperature gradient along optical fibre path. These fluctuations in the optical fibre response follow no clear pattern which is an indicator of no hotspot in the superconductor.

### 4.2. Experiment results for 7 K temperature change

For this experiment 450 A was applied to the sample for 50 ms, as shown by blue curve in figure 4(b). This figure also shows the temperature curve measured by the PT1000, with the maximum temperature change  $\approx 7$  K. The oscillatory response of the optical fibre, shown in red, can be seen to vary in frequency according to the temperature change in figure 4(b). Figure 4(c) shows an enlarged view of the same graph for the duration of the current pulse. It shows that the voltage around the hotspot,  $v_{3-4}$ , (shown in black in figure 4(c)) reaches 0.8 V while in the adjacent segments ( $v_{1-2}$ ) and ( $v_{5-6}$ ) it remains zero. These zero voltages in adjacent segments signify the presence of a single point of heating in the sample. Before the voltage begins to rise around the hotspot, the optical fibre response shows no clear pattern which can be observed in figure 4(c) up to 30 ms after the pulse. In the presence of a

hotspot, the optical fibre response shows a rapid transition to an oscillatory response of the form  $\cos(\Delta\phi_H)$  as explained in the theoretical analysis. The optical fibre response is rapid and oscillations are observed as soon as voltage around the weak point begins to rise. It is interesting to note that the thermometer begins to show a temperature increase 20 ms after the oscillatory response is observed in the optical fibre output. This delay in the thermometer response as compared to the optical fibre response can be explained by the fact that thermal transfer is slower than strain transfer to the optical fibre. The technique therefore is sensitive to both temperature and strain which highlights the importance of understanding the setup sensitivity to achieve a more rapid response to hotspots.

### 4.3. Optical fibre sensitivity in cryogenic temperatures

It was highlighted in section 2 that the composite optical fibre response comprises of a strain response and a thermal response. The optical fibre thermal sensitivity is defined by two key parameters: the thermo-optic coefficient ( $\xi$ ) and the thermal expansion coefficient ( $\alpha_o$ ), which contributes to the temperature dependent term in equation (2). In the thermal response at room temperature,  $\xi$  plays a more significant role as compared to  $\alpha_o$ , owing to the very low thermal expansion of the optical fibre material, silica. At cryogenic temperatures however, it has been experimentally demonstrated that the thermal sensitivity reduces due to a sharp decrease in  $\xi$ : the value of  $\xi$  is  $9 \times 10^{-6} \text{ K}^{-1}$  at room temperature which decreases by three times to  $3 \times 10^{-6} \text{ K}^{-1}$  at 77 K [18]. For improving thermal sensitivity, approaches of recoating optical fibres with metallic or polymer coatings to enhance the thermal expansion coefficient have been studied for techniques like FBG [19]. It has also been discovered in studies that the overall decrease in the temperature sensitive term ( $\alpha_o + \xi$ ) makes it possible to perform strain dominated measurements at cryogenic temperatures [20]. The strain sensitivity, is dominated by strain imposed on the optical fibre due to the thermal contraction or expansion of the host material, in this case the Hastelloy. For high strain sensitivity the integration of the optical fibre to the superconductor needs to be appropriate to maximise strain transfer from the host material to the optical fibre. It should be noted that the strain is transferred from the Hastelloy to the STYCAST<sup>®</sup> and then to the optical fibre. It was discussed in section 3 that there is only a small difference between the coefficient of thermal expansion of STYCAST<sup>®</sup> and the HTS tape; this ensures good strain transfer. When the optical fibre is placed directly above the Hastelloy stabilizer in thermally stabilized tapes, the delay in hotspot detection increases in the case of thermal coupling because of the increased distance to the optical fibre, but remains unchanged in case of strong mechanical coupling with good strain transfer; this will be further discussed in future publications. Experiments have been carried out to investigate the response time of our technique to the hotspots by exploring different options for optical fibre coupling, but

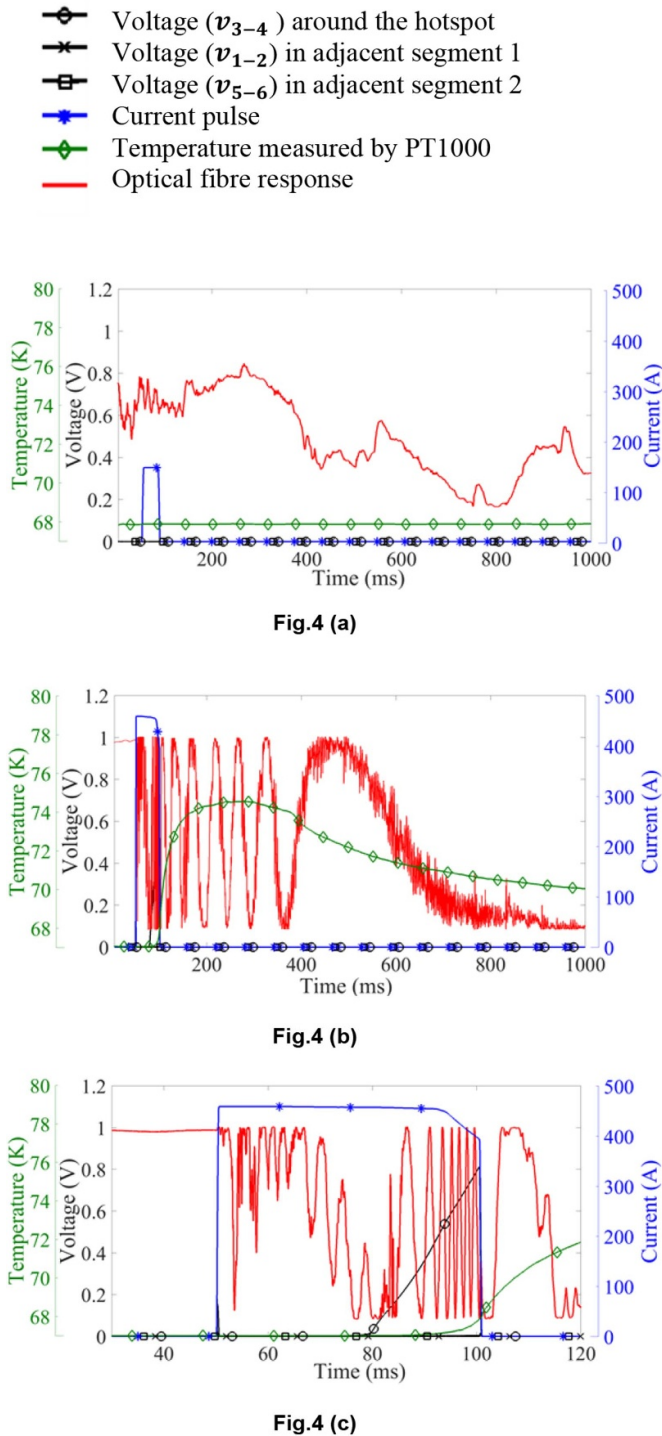


**Figure 4.** (a) Experiment results for no hotspot, the MZI response shows slow variations with no visible pattern (b) The technique detects a single hotspot in the superconductor, temperature curve and corresponding optical fibre response for which is observed (c) A closer look at figure 4(b) shows the optical fibre’s instantaneous oscillatory response to the hotspot, as voltage around the hotspot begins to rise.

ongoing and future work on this technique aims at exploring various integration techniques for better strain sensitivity in MZI.

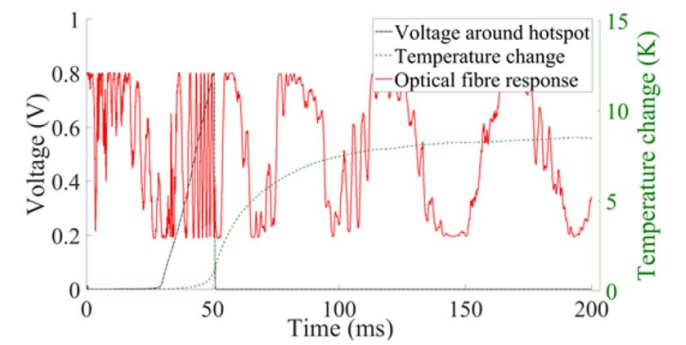
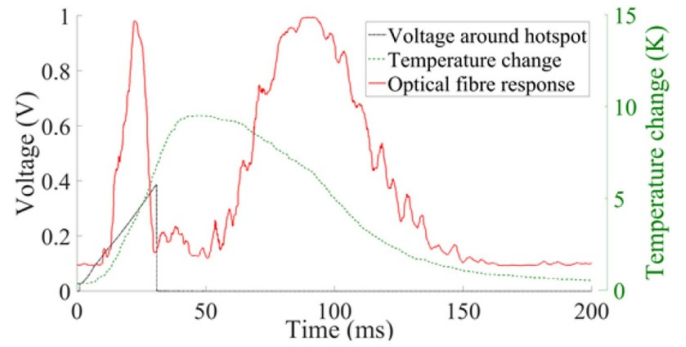


**Figure 5.** Comparison of the technique response to same temperature change of  $\sim 10$  K produced by current pulse applied at  $t = 0$  ms (a) Exp 1: The setup sensitivity is lowered due to a weak optical fibre coupling with the sample (b) Exp 2: Strong mechanical coupling between the sample and optical fibre allows a stronger strain sensitive response that is observed before the temperature increase in the PT1000.

**Table 1.** Specifications of Exp 1 and Exp 2.

Experiment	Optical fibre coupling	Response
Exp 1.	Thermal only	Temperature sensitive (Low sensitivity, slow)
Exp 2.	Strong mechanical and thermal	Strain dominated (High sensitivity, fast)

#### 4.4. Experimental setup sensitivity

In the experiment results from figure 4, it is demonstrated that the technique is capable of detecting a singular hotspot immediately, however in our experiments it has been observed that the setup sensitivity is not constant and varies depending on multiple factors like the quality of the optical fibre integration, liquid nitrogen bath temperature and sample type.

In this section, we focus on investigating how the sensitivity and response time depends on the kind of coupling present between the optical fibre and the conductor. Table 1 characterizes two experimental setups, identified as Exp 1 and Exp 2, that varied in terms of optical fibre coupling to

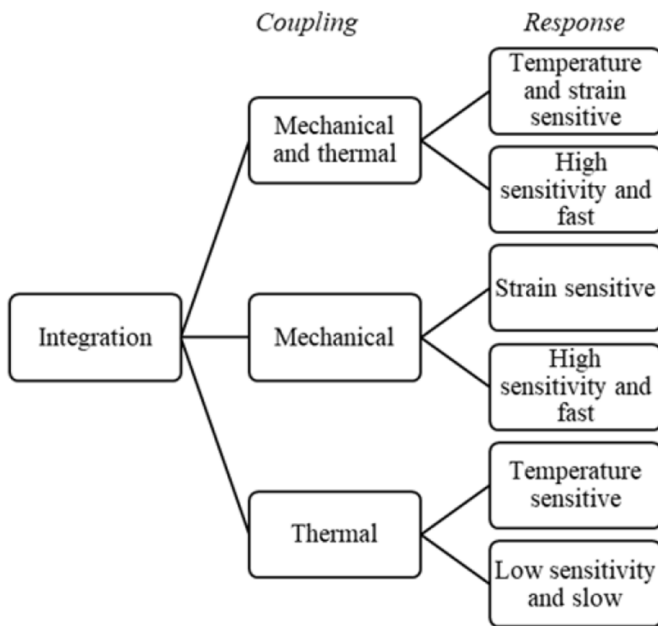


**Figure 6.** Dependence of the technique response on quality of integration.

the sample. In order to create thermal coupling, a mechanically soft coupling is required; the media used for integration should remain soft but conduct the heat. For Exp 1, excessive catalyst is added to STYCAST<sup>®</sup> leading to a soft malleable finish that weakens strain transfer to the optical fibre leading to a predominantly thermal coupling. For Exp 2, less catalyst is used in STYCAST<sup>®</sup> preparation for a hard, rigid finish that maximises strain transfer to the optical fibre, ensuring a strong mechanical as well as thermal coupling. It should be noted that two different samples were used for the experiments. A comparison of the response of the technique in the two experiments for a 10 K temperature change measured by the PT1000, are shown in figures 5(a) and (b), respectively.

From figures 5(a) and (b) it is observed that the hotspot begins to form around 0 ms for Exp 1 and at 30 ms for Exp 2, as the voltage around the hotspot begins to rise (shown in black). The hotspot onset and hotspot voltage are different in the two experiments, due to the samples being different in terms of critical current variation.

It can be observed in figure 5(a) that Exp 1 shows a weak, low frequency response to the hotspot. Due to impeded strain transfer to the optical fibre, the response in Exp 1 is mainly due to a slow thermal transfer to the optical fibre. However, for the same temperature change a much stronger response is observed for Exp 2, as shown in figure 5(b) where the optical fibre response precedes the PT1000 temperature increase by  $\sim 20$  ms. This signifies that the response is due to thermally induced strain in the sample, which can be observed before a temperature change is observed by the thermometer. Experimental results demonstrate that, proper mechanical coupling between the optical fibre and the superconductor can enhance the sensitivity of the setup to thermally-induced strains, leading not only to a more

instantaneous strain-dominated response but also enabling lower temperature hotspot detection, as summarized in Figure (6).

## 5. Conclusion

This optical fibre sensing technique developed at EPFL for hotspot detection in SFCLs enables extremely fast hotspot detection. It has been experimentally demonstrated that our technique can detect even singular hotspots along the superconductor length, within 10 ms. This technique is not only fast but also extremely cost effective, making it a significant breakthrough for not only SFCLs but also other HTS applications. Work is being carried out on this technique to achieve the highest sensitivity and lowest response time, but these initial results provide promising prospects of a reliable health monitoring system, to supplement HTS applications and to ensure resilience against hotspots and thermal runaways.

## Acknowledgments

This project has received funding from the European Union's Horizon 2020 research and innovation programme under grant agreement no. 721019.

## ORCID iDs

Arooj Akbar  <https://orcid.org/0000-0003-1779-4540>  
Zhisheng Yang  <https://orcid.org/0000-0002-6617-4623>

## References

- [1] Debnath S and Chinthavali M 2017 Control of MMC-HVDC in low-inertia weak grids *2017 IEEE 12th Int. Conf. on Power Electronics and Drive Systems (PEDS)* pp 435–41
- [2] Ervin S, Dominik E, Cora P and Frank S J D 2016 A closer look at protection concepts for DC systems *CIGRE B4-118*
- [3] Leon Garcia W R, Tixador P, Raison B, Bertinato A, Luscan B and Creusot C 2017 Technical and economic analysis of the R-type SFCL for HVDC grids protection *IEEE Trans. Appl. Supercond.* **27** 5602009
- [4] Chen L, Tang F and Ren L 2016 Comparative study of inductive and resistive SFCL to mitigate the DC fault current in a VSC-HVDC system integrated with wind power farms *2015 Int. Conf. Applied Superconductivity and Electromagnetic Devices, ASEM 2015 - Proc.* pp 64–65
- [5] Noe M, Hobl A, Tixador P, Martini L and Dutoit B 2012 Conceptual Design of a 24 kV, 1 kA Resistive Superconducting Fault Current Limiter *IEEE Trans. Appl. Supercond.* **22** 5600304
- [6] Tixador P et al 2019 Status of the european union project FASTGRID *IEEE Trans. Appl. Supercond.* **29** 5603305
- [7] Gömöry F, Šouc J, Adánek M, Ghabeli A, Solovyov M and Vojeníak M 2019 Impact of critical current fluctuations on the performance of a coated conductor tape *Supercond. Sci. Technol.* **32** 124001
- [8] Kraemer H P, Schmidt W, Utz B and Neumueller H W 2003 Switching behavior of YBCO thin film conductors in

- resistive fault current limiters *IEEE Trans. Appl. Supercond.* **13** 2044–7
- [9] Lacroix C, Fournier-Lupien J H, McMeekin K and Sirois F 2013 Normal zone propagation velocity in 2g hts coated conductor with high interfacial resistance *IEEE Trans. Appl. Supercond.* **23** 3–7
- [10] Búran M, Vojenčiak M, Moša M, Ghabeli A, Solovyov M, Pekarčíková M, Kopera J and Gömöry F 2019 Impact of a REBCO coated conductor stabilization layer on the fault current limiting functionality *Supercond. Sci. Technol.* **32** 095008
- [11] Fournier-Lupien J H, Lacroix C, Hellmann S, Huh J, Pfeiffer K and Sirois F 2018 Use of the buffer layers as a current flow diverter in 2G HTS coated conductors *Supercond. Sci. Technol.* **31** 125019
- [12] Justin S, Federico S and Rogers Samuel C W K 2017 United States Patent Application Publication Schwartz et al
- [13] Alvarez-Botero G, Baron F E, Cano C C, Sosa O and Varon M 2017 Optical sensing using fiber bragg gratings: Fundamentals and applications *IEEE Instrum. Meas. Mag.* **20** 33–38
- [14] Yang Zhisheng A A 2020 Hotspot Monitoring System for Superconducting Device, International Patent Application n° PCT/IB2020/058039
- [15] Kersey A D, Davis M A, Patrick H J, LeBlanc M, Koo K P, Askins C G, Putnam M A and Friebele E J 1997 Fiber grating sensors *J. Light. Technol.* **15** 1442–62
- [16] Bagrets N, Otten S, Weiss K P, Kario A and Goldacker W 2015 Thermal and mechanical properties of advanced impregnation materials for HTS cables and coils *IOP Conf. Ser. Mater. Sci. Eng.* **102** 012021
- [17] Liang F, Venuturumilli S, Zhang H, Zhang M, Kvitkovic J, Pamidi S, Wang Y and Yuan W 2017 A finite element model for simulating second generation high temperature superconducting coils/stacks with large number of turns *J. Phys. D: Appl. Phys.* **122** 043903
- [18] Scurti F, McGarrahan J and Schwartz J 2017 Effects of metallic coatings on the thermal sensitivity of optical fiber sensors at cryogenic temperatures *Opt. Mater. Express* **7** 1754
- [19] Chiuchiolo A, Bajko M, Perez J C, Bajas H, Consales M, Giordano M, Breglio G and Cusano A 2014 Fiber bragg grating cryosensors for superconducting accelerator magnets *IEEE Photonics J.* **6** 1–10
- [20] Rajini-Kumar R, Suesser M, Narayankhedkar K G, Krieg G and Atrey M D 2008 Performance evaluation of metal-coated fiber Bragg grating sensors for sensing cryogenic temperature *Cryogenics (Guildf)* **48** 142–7